Boost the Adversarial Learning with Fourier Regulator: Bias-field Correction on MRI

Tong Li*[a], Anran Liu*[b], David Kügler[c], and Martin Reuter[c,d,e]

[a]Division of Computational Data Sciences, Washington University in St. Louis, St. Louis, USA
[b]Department of Health Technology and Informatics, The Hong Kong Polytechnic University, Hong Kong, Hong Kong SAR, China
[c]AI in Medical Imaging, German Center for Neurodegenerative Diseases (DZNE), Bonn, Germany
[d]A.A. Martinos Center for Biomedical Imaging, Massachusetts General Hospital, Boston, USA
[e]Department of Radiology, Harvard Medical School, Boston, USA

ABSTRACT

In magnetic resonance imaging, signal intensity inhomogeneities due to intrinsic bias field pose a significant challenge for automated medical image analysis. Conventional methods to mitigate these effects, such as N4ITK, are time-consuming and unstable. The exploration of deep learning alternative approaches is still at an unknown stage. Previous studies have obtained preliminary results in GAN-based models, but we found the difficulty in aligning bias-corrected image domains with clean image domains during adversarial learning may affect the retention of normal organizational structures. Therefore, we propose a novel Fourier regulator structure that can be integrated into the general adversarial learning framework. It explicitly decouples different levels of semantic features based on the Fourier field and utilizes explicit feature learning to enhance intrinsic coherence and promote more organized domain alignment. By separating amplitude and phase features as well as splitting low and high-frequency information, our model preserves organizational details more efficiently and explicitly separates intensities across organizational boundaries. During the training process of adversarial learning, the generator generates the target domain while the regulator and discriminator are fixed; the regulator and discriminator are updated in parallel while the generator is fixed. Such a learning approach extends the original min-max optimization problem of adversarial learning to a multi-player mix-max optimization problem. The discriminator can quickly draw the generative domain closer to the target domain, while the regulator aligns the distance to the target domain in a more explicit feature-learning manner. Evaluated on the OASIS and BrainWeb datasets, our model outperforms traditional and deep learning methods to enhance homogeneity. It also shows consistent performance in other image reconstruction tasks, demonstrating its generalization capabilities.

1. INTRODUCTION

MRI usually has the problem of inherent intensity non-uniformity (INU), which can introduce variances within the measured signal intensity from homogeneous tissue. Conventional methods face challenges such as long computational times,[1] especially for SPM, and diminished efficacy in correcting strong bias fields when operating the N4/N3 method.[2] Recent developments have introduced deep neural networks for bias field correction, such as cascaded convolutional networks or generative models, including GANs,[2–4] to address bias fields from a domain transformation perspective. However, our experimental analyses of certain GAN-based models reveal challenges in aligning the corrected Intensity Non-Uniformity (INU) domain which is built from a generator and Bias Field Uniform (BNU) target domain. This can impact the effectiveness of bias field correction and the ability to maintain tissue consistency. In this paper, we propose a regularization scheme in the Fourier field for

*Tong Li and Anran Liu contributed equally to this paper
Tong Li: E-mail: li.tong@wustl.edu
Martin Reuter: E-mail: martin.reuter@dzne.de

Medical Imaging 2025: Image Processing, edited by Olivier Colliot, Jhimli Mitra, Proc. of SPIE Vol. 13406, 134060Y · © 2025 SPIE
1605-7422 · doi: 10.1117/12.3047299

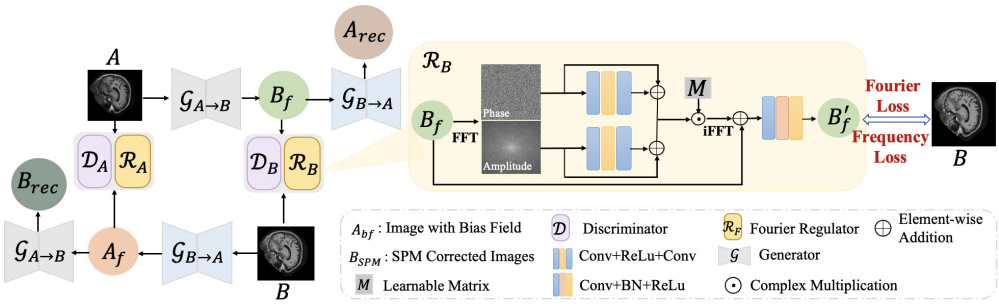

Figure 1: The overall architecture of CycleGAN with Fourier regulation scheme. The Regulator $\mathcal{R}_B$ operates in parallel with $\mathcal{D}_B$, employs decoupled feature learning from predictions B_f and coordinates with the joint loss with Fourier and Frequency losses, enabling domain alignment and optimizing the transformation process between the INU and BFU domains.

explicit feature learning and domain alignments at different spatial levels in the GAN-structure model. This regularization runs in parallel with the discriminator, so we refer to it as the regulator below. It first decouples and processes the amplitude and phase information of the Fourier field, leveraging the correlation between spatial features and Fourier components. The separate learning of Fourier components and the designed respective loss functions aid in decoupling different levels of information (high-level semantic information and low-level stylistic information) and guide a more explicit and structured feature learning and domain alignment, also facilitating the generators to have more objective updates. We conducted experiments on bias field correction tasks to demonstrate that our proposed method outperforms other methods while maintaining high model efficiency.

2. METHOD

Building on the GAN approach, our model interleaves two generator-discriminator pairs for image-image transformation and incorporates an additional parallel regulator to assist discriminators in maintaining intrinsic consistency in domain transformation, shown in Fig. 1. We denote the two image domains by A and B which represent the INU (Intensity Non-Uniformity) and BFU (Bias Field Uniform) domains, respectively. A basic CycleGAN model uses a generator $\mathcal{G}_{A\to B}$ to transform images from A to B, generating the synthetic bias-field corrected image B_f from A and reconstructed bias-field corrected image B_{rec} from A_f, as well as an inverse generator $\mathcal{G}_{B\to A}$. In regulator $\mathcal{R}_B$, the input B_f is first decoupled into phase and amplitude components. Subsequently, a series of convolution operations and a learnable matrix M perform feature learning on the Fourier domain. Then, the Fourier information, enriched by explicit feature learning, is transformed back into the image domain and aligned with paired images of the dataset (here B) using a custom-tailored combination of Fourier loss and frequency loss. The same corresponding operations are also implemented in $\mathcal{R}_A$. This enhances the CycleGAN network with explicit feature learning and regularization using Fourier information.

2.1 Regularization via Fourier Space

Inspired by some other work on natural images,[5,6] we found that the phase component of the Fourier spectrum tends to preserve the high-level semantic structure, and the amplitude component contains the style information. Therefore, motivated by the perspective in Fourier space, we try to decouple amplitude and phase components and conduct separate feature mining in both domains to alter the style changes the bias field brings while mitigating the loss of the high-level semantics in MRI. Therefore, we propose that the Fourier Regulator be used to give explicit feature regularization on domains and the network. Given an image with bias field $x \in \mathcal{A}$ ($\mathcal{A} \in \mathbb{R}^{H\times W\times 3}$), the generator $\mathcal{G}_{A\to B}$ transforms x to a fake field B_f. For each channel, we conduct the Fourier transform $\mathcal{F}(x)$ and obtain the two components in the frequency domain, amplitude $\mathcal{A}(x)$ and phase$\mathcal{P}(x)$. To capture different levels of features of MRI as discussed before, we respectively apply convolutional operations and residual connections on phase and amplitude components. After the separate feature learning on amplitude and phase, we can obtain the updated Fourier representation. The learned $\mathcal{F}(x)$ can be calculated by the updated $\mathcal{A}$ and $\mathcal{P}$.

Further, we perform feature learning at the global Fourier information level. Inspired by,[7] we apply a learnable kernel matrix M point-wise on the Fourier features $\mathcal{F}(x)$, instead of convolutions, to obtain feature information

Table 1: Evaluations on BrainWeb with low and high bias field strength.

	BF-strength		N4[9]	U-Net[10]	Pix2pix[11]	CycleGAN[8]	Diffusion[12]	ScrNet[13]	ABCNet[2]	Ours
T1	Low	SSIM	0.9821	0.9795	0.8535	0.9829	0.9723	0.9788	0.9901	**0.9940**
		PSNR	37.6654	37.2301	30.0753	37.9950	37.4385	37.0923	37.2650	**39.0848**
	High	SSIM	0.9366	0.9640	0.9021	0.9560	0.9671	0.9701	0.9743	**0.9935**
		PSNR	32.3682	33.9726	32.0378	34.2631	37.9503	38.7824	36.3291	**40.2531**
T2	Low	SSIM	0.9730	0.9567	0.8935	0.9632	0.9789	0.9858	0.9867	**0.9907**
		PSNR	34.0923	32.0057	30.0729	32.0219	34.4080	35.0097	**37.0601**	36.0590
	High	SSIM	0.9081	0.9534	0.8900	0.9302	0.9739	0.9811	0.9728	**0.9843**
		PSNR	29.5742	30.4502	30.7826	32.0247	33.4421	33.8660	32.8652	**34.4720**

Table 2: Evaluations on Oasis

Method	SSIM	PSNR
N4[9]	0.9422	32.9966
U-Net[10]	0.9173	32.6853
Pix2pix[11]	0.8115	31.6418
CycleGAN[8]	0.9202	33.2741
Diffusion[12]	0.8960	33.9893
ScrNet[13]	0.8897	**34.8525**
Ours	**0.9650**	34.2646

globally over the Fourier field. The Fourier feature $\mathcal{F}(x)$ performs a complex multiplication for each channel with the kernel matrix $M \in \mathbb{C}^{H\times W}$ of the same size as the input x. Hence, for example, given $\mathcal{F}(x) = A + Bj$ and $M = C + Dj$ ($\mathcal{F}(x) \in \mathbb{C}, M \in \mathbb{C}$), the feature learning developed by the matrix kernel and point-wise multiplication in Fourier space can be expressed as

$$\mathcal{F}(x) \times M = (AC - BD) + (AD + BC)j. \tag{1}$$

Finally, through the iFFT and a series of residual and convolution operations, we obtain features based on Fourier information after amplitude and phase decoupled learning and convolution learning in different dimensions of the Fourier and spatial fields.

2.2 Loss Functions

Consistent with the loss function of the CycleGAN structure, we utilize the same loss functions in discriminator and combine our designed loss in the generator, which can be formulated as:

$$\mathcal{L}_{gen,A\to B} = \mathcal{L}_{GAN,A} + \lambda_{Regulator}\mathcal{L}_{Regulator,A} + \lambda_{cyc}\mathcal{L}_{cyc,A} + \lambda_{idt}\mathcal{L}_{idt,A}, \tag{2}$$

where $\mathcal{L}_{GAN}$, $\mathcal{L}_{cyc}$, $\mathcal{L}_{idt}$ are consistent with CycleGAN model,[8] $\lambda_{Regulator}$, λ_{cyc} and λ_{idt} are combination coefficients. $\ell_{Regulator}$ is the loss function in the Fourier regulator. And $\mathcal{L}_{gen,A\to B}$ utilizes the same loss functions. In the Regulator loss function, in order to facilitate the explicit feature alignment and reduce the distance between the fake (A_f/B_f) images generated by the generator and the corresponding reference (A/B) domain images, we use a hybrid loss based on $L1$ regression loss $\mathcal{L}_{reg}$, frequency information $\mathcal{L}_{Freq}$ and Fourier field information $\mathcal{L}_{fft}$ to enhance the learning progress as much as possible.

$$\mathcal{L}_{Regulator,A/B} = \lambda_1\mathcal{L}_{reg,A/B} + \lambda_2\mathcal{L}_{Freq,A/B} + \lambda_3\mathcal{L}_{fft,A/B} \tag{3}$$

where λ_1, λ_2 and λ_3 are adjustable parameters. The frequency loss function is calculated based on separated low-frequency and high-frequency information of the images. In the Fourier loss function, for the output of the regulator, the current amplitude and phase information are first obtained after FFT and then paired with the corresponding real value of the domain for the calculation of the loss calculation

$$\mathcal{L}_{fft,B} = \mathbb{E}_{x\sim A}(\ell_{reg}(Amp(B_{\text{ref}}), Amp(\mathcal{R}_B(\mathcal{G}_{A\to B}(x)))) \tag{4}$$

$$+ \ell_{reg}(Pha(B_{\text{ref}}), Pha(\mathcal{R}_B(\mathcal{G}_{A\to B}(x))))), \tag{5}$$

where B_{ref} is the reference images. And $\mathcal{L}_{fft,A}$ can be obtained in a similar way.

3. EXPERIMENTS

In the evaluation of our proposed method, we utilized two significant datasets: the BrainWeb Dataset * and raw data in the Oasis1 Data.[14] In the BrainWeb dataset, we specifically chose T1 and T2 sequences with 1mm slice thickness and 0% noise, targeting both low (20%-40%) and high (40%-68%) intensity non-uniformity levels. The BrainWeb data with 0% intensity non-uniformity was used as the ground truth for bias-field correction. In the Oasis dataset, we utilized the SPM bias-corrected images as the reference standard.

*http://www.bic.mni.mcgill.ca/brainweb/.

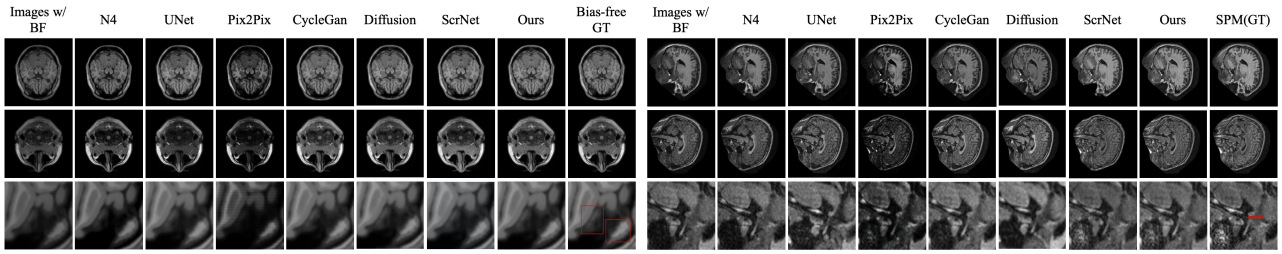

(a) Visual comparison on BrainWeb. (b) Visual comparison on Oasis.

Figure 2: Visual comparison of the results

Table 3: Organization Comparison Results

	GM-SSIM	WM-SSIM	CSF-SSIM
Original	1.000±0.000	1.000±0.000	1.000±0.000
w/ Bias Field	0.931±0.025	0.911±0.064	0.927±0.046
N4[9]	0.965±0.031	0.961±0.032	0.941±0.023
U-Net[10]	0.954±0.030	0.926±0.027	0.923±0.028
Diffusion[12]	0.962±0.011	0.950±0.015	0.945±0.017
ScrNet[13]	0.975±0.014	0.963±0.019	**0.971±0.027**
Ours	**0.989±0.008**	**0.981±0.010**	0.969±0.022

Table 4: Fundus Image Enhancement

Method	SSIM	PSNR
U-Net[10]	0.8426	20.1804
CycleGAN[8]	0.8370	20.0922
ScrNet[13]	**0.9119**	**27.4997**
Ours	0.8835	25.1740

In the experiments, we compared our method to the popular N4 method[9] and the following deep learning-based models: U-Net,[10] Pix2pix,[11] CycleGAN,[8] ScrNet,[13] Diffusion model[12] and ABCNet.[2] ScrNet is designed to enhance the image of the cataract fundus. In the Diffusion model, we continuously perturb the image by adding Gaussian noises. Besides, we didn't compare ABCNet in Oasis because it requires the ground truth of the bias field. Table 1 presents a comparison of bias-field correction results on the BrainWeb dataset. The results indicate that corrected MRI scans show better intensity uniformity across tissue classes. And we can see that the N4 method effectively handles low-bias fields but struggles with higher intensities. U-Net and CycleGAN had good results but also slightly varied with bias-field intensity. In contrast, the Diffusion model, ScrNet, and ABCNet demonstrated stable performance. Our model achieved the best and most stable results in nearly all experiments. In the Oasis results, shown in Table 2, we observed that N4's effectiveness was reduced compared to its performance on the BrainWeb data. While all models have some degree of performance degradation, ScrNet has a more obvious drop. The evaluation result of our model on SSIM is still competitive. Fig. 2a and Fig. 2b show exemplary results on BrainWeb and Oasis datasets, respectively, along with close-up details. These figures show that the real bias fields in Oasis are less prominent than the simulated ones in BrainWeb. However, both datasets exhibit significantly improved intensity uniformity and enhanced contrast between different tissue classes after correction. Additionally, the close-up views highlight that our method best preserves structural details in both datasets. Additionally, we conduct downstream tasks on the segmentation of Gray matter (GM), White matter (WM), and Cerebrospinal fluid (CSF), and compare the similarity of correction results in the Brainweb dataset and clean image for different organizations respectively. We conduct extra experiments on fundus image enhancement to test the generalizability of our model. Shown in Table 3 and Table 4, the highest organizational similarity reinforces the validity of our model and generalization experiments on fundus image enhancement demonstrate that our model retains strong performance across different imaging modalities.

4. CONCLUSION

We propose a generic enhancement network based on the GAN structure to robustly correct bias fields in MRI. Our model, featuring a Fourier regulator architecture that collaborates with a GAN discriminator, explicitly decouples different levels of semantic features based on the Fourier field. This addresses the learning limitations of deep neural networks and domain alignment difficulties. Comprehensive experiments on synthetic and real imaging data demonstrate the effectiveness and generalizability of our model. Additionally, we demonstrate the generalization of our approach to fundus image intensity correction.

Acknowledgments This work has not been submitted for publication or presentation elsewhere.

REFERENCES

[1] Simko, A., ofstedt, T. L., Garpebring, A., Nyholm, T., and Jonsson, J., "Mri bias field correction with an implicitly trained cnn," in [*Proc. PMLR*], 1125–1138 (2022).

[2] Chen, L., Wu, Z., Hu, D., Wang, F., Smith, J., and Lin, W., "Abcnet: Adversarial bias correction network for infant brain mr images," *Med. Image Anal.* **72**, 102133 (2021).

[3] Dai, X., Lei, Y., Liu, Y., Wang, T., Ren, L., Curran, W. J., Patel, P., Liu, T., and Yang, X., "Intensity non-uniformity correction in mr imaging using residual cycle generative adversarial network," *Phys. Med. Biol.* **65**(21) (2020).

[4] Lee, J., Kang, J., Nam, Y., and Lee, T., "Bias field correction in mri with hampel noise denoising diffusion probabilistic model," in [*Proc. MIDL*], (2023).

[5] Hoang, T., Zhang, H., Yazdani, A., and Monga, V., "Transer: Hybrid model and ensemble-based sequential learning for non-homogenous dehazing," in [*Proc. CVPR*], 1670–1679 (2023).

[6] Weiyi, Y., Lei, L. Y., and Hongming, S., "Fan-net: Fourier-based adaptive normalization for cross-domain stroke lesion segmentation," in [*Proc. ICASSP*], 1–5 (2023).

[7] Han, Y. and Hong, B., "Deep learning based on fourier convolutional neural network incorporating random kernels," *Electronics* **10**(16), 2004 (2021).

[8] Zhu, J., Park, T., Isola, P., and Efros, A., "Unpaired image-to-image translation using cycle-consistent adversarial network," in [*Proc. ICCV*], 2223–2332 (2017).

[9] Tustison, N. and Gee, J., "N4itk: Nick's n3 itk implementation for mri bias field correction," *Insight* **9** (2009).

[10] Ronneberger, O., Fischer, P., and Brox, T., "U-net: Convolutional networks for biomedical image segmentation," in [*Proc. MICCAI*], 234–241 (2015).

[11] Isola, P., Zhu, J., Zhou, T., and Efros, A., "Image-to-image translation with conditional adversarial networks," in [*Proc. CVPR*], 1124–1134 (2017).

[12] Khader, F., Müller-Franzes, G., Arasteh, S., Han, T., Haarburger, C., Schulze-Hagen, M., Schad, P., Engelhardt, S., Baeler, B., Foersch, S., Stegmaier, J., Kuhl, C., Nebelung, S., Kather, J., and Truhn, D., "Denoising diffusion probabilistic models for 3d medical image generation," *Sci Rep* **13**(7303) (2023).

[13] Li, H., Liu, H., Fu, H., Shu, H., Zhao, Y., Luo, X., Hu, Y., and Liu, J., "Structure-consistent restoration network for cataract fundus image enhancement," in [*Proc. MICCAI*], 487–496 (2022).

[14] Marcus, D., Wang, T., Parker, J., Csernansky, J., Morris, J., and Buckner, R., "Open access series of imaging studies (oasis): cross-sectional mri data in young, middle aged, nondemented, and demented older adults," *J. Cogn. Neurosci.* **19**(9), 1498–1507 (2007).